Grid Cells and Spatial Maps in Entorhinal Cortex and Hippocampus

Tor Stensola and Edvard I. Moser

Abstract The cortical circuit for spatial representation has multiple functionally distinct components, each dedicated to a highly specific aspect of spatial processing. The circuit includes place cells in the hippocampus as well as grid cells, head direction cells and border cells in the medial entorhinal cortex. In this review we discuss the functional organization of the hippocampal-entorhinal space circuit. We shall review data suggesting that the circuit of grid cells has a modular organization and we will discuss principles by which individual modules of grid cells interact with geometric features of the external environment. We shall argue that the modular organization of the grid-cell system may be instrumental in memory orthogonalization in place cells in the hippocampus. Taken together, these examples illustrate a brain system that performs computations at the highest level, yet remains one of the cortical circuits with the best readout for experimental analysis and intervention.

Place Cells and Grid Cells

An entirely new branch of neuroscience opened with the discovery of hippocampal place cells, i.e., cells that fire specifically when animals are in certain locations (O'Keefe and Dostrovsky 1971; O'Keefe and Nadel 1978; Fig. 1). Different place cells were found to fire in different locations of the environment (O'Keefe 1976), such that, for any given ensemble of place cells, the animal's location could be decoded from the pattern of activity among those cells (O'Keefe and Nadel 1978; Wilson and McNaughton 1993). With these insights, place cells became a strong

T. Stensola
Kavli Institute for Systems Neuroscience and Centre for Neural Computation, Norwegian University of Science and Technology, Olav Kyrres gate 9, 7491 Trondheim, Norway

Champalimaud Neuroscience Programme, Champalimaud Centre for the Unknown, Lisbon 1400-038, Portugal

E.I. Moser (✉)
Kavli Institute for Systems Neuroscience and Centre for Neural Computation, Norwegian University of Science and Technology, Olav Kyrres gate 9, 7491 Trondheim, Norway
e-mail: edvard.moser@ntnu.no

G. Buzsáki, Y. Christen (eds.), *Micro-, Meso- and Macro-Dynamics of the Brain*, Research and Perspectives in Neurosciences, DOI 10.1007/978-3-319-28802-4_5

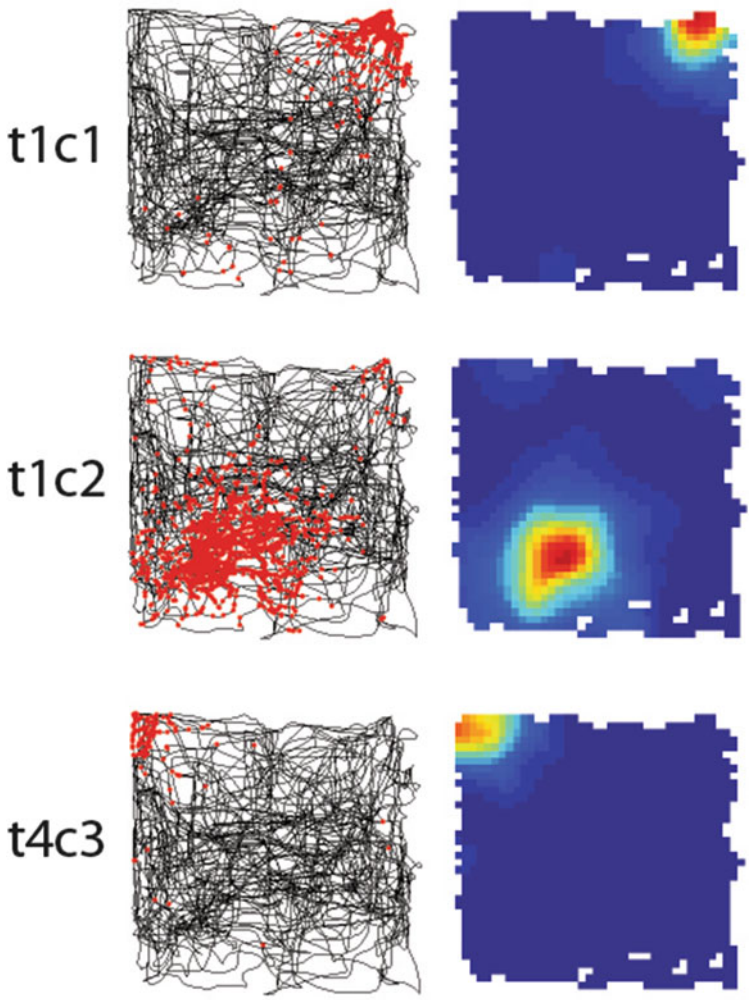

Fig. 1 Place cells recorded in hippocampal subarea CA3. Bird's eye view of firing locations of three place cells, with firing locations shown as *red dots* on the path of the rat (*black*). *t* indicates tetrode number, *c* cell number. Cells were recorded simultaneously. *Right*: pseudo-color activity maps of the cells to the left. *Red* is high firing rate, and *blue* is no firing. Reproduced with permission from Fyhn et al. (2007)

candidate for the neural implementation of Tolmanian cognitive maps, maps that animals use to guide their navigation in the environment (Tolman 1948; O'Keefe and Nadel 1978).

In trying to understand which incoming signals could take part in generating location-specific responses in place cells, both experimental and theoretical suggestions have been presented. An important clue was the experimental

demonstration that place cells in CA1 could sustain place characteristics after ablation of all input from CA3 (Brun et al. 2002). This observation suggested that place responses in CA1 originated from an alternative source of excitatory input to CA1: the medial entorhinal cortex (MEC). In pursuing this possibility, we observed that neurons in MEC were also spatially selective (Fyhn et al. 2004; see also Hargreaves et al. 2005), although MEC neurons typically had several firing fields in environments where place cells had only a single field. It turned out that the firing fields of the spatial cells in MEC formed a near-perfect hexagonal grid tessellating the entire space available to the animal (Hafting et al. 2005; Fig. 2). Each grid cell had a slightly different set of *x*, *y*-coordinates in the environment, so that the entire environment could be covered collectively by a small number of grid cells. Dorsally in MEC, grid patterns typically had small fields packed densely together. At more ventral MEC locations, with increasing distance from the dorsal MEC border, the scale of the grid pattern expanded (Fyhn et al. 2004; Hafting et al. 2005; Brun et al. 2008; Fig. 2). Several computational models (O'Keefe and Burgess 2005;

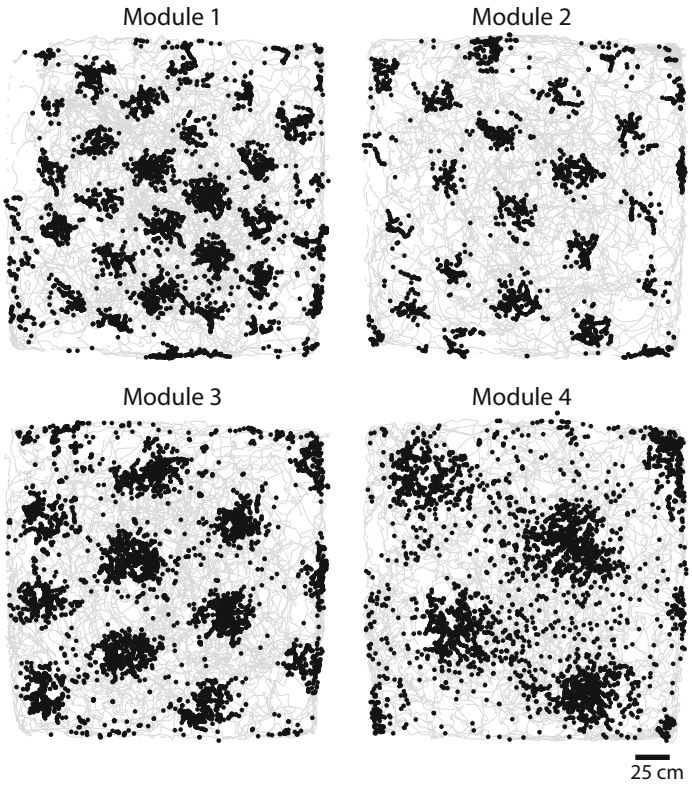

Fig. 2 Grid cell firing patterns; bird's eye view. Action potentials (*black*) superimposed on the movement path (*gray*) reveal a periodic spatial activity pattern. Shown are grid patterns of four distinct scales recorded within the same animal. Reproduced with permission from Stensola et al. (2012)

Fuhs and Touretzky 2006; McNaughton et al. 2006; Burak and Fiete 2009; Burgess et al. 2007) and multiple lines of experimental evidence (Brun et al. 2002; Van Cauter et al. 2008; Zhang et al. 2013) soon pointed to grid cells as prime candidates in conferring spatial selectivity to place cells in downstream hippocampus.

Models that describe possible grid-to-place transforms are dependent on how the grid map is organized at several functional levels. Grid spacing is organized topographically along the dorsoventral axis of MEC, with average grid spacing increasing from dorsal to ventral (Fyhn et al. 2004; Hafting et al. 2005; Brun et al. 2008). Despite initial reports based on low cell numbers (Barry et al. 2007), it remained unclear after the first studies whether grid scale distributed within animals as a scale-continuum or instead progressed in steps. To answer this question, it was essential to record large numbers of grid cells over considerable dorsoventral distances within animals, so as to sample a sufficient range of grid spacing. It was necessary to record with minimal discontinuity in the tissue so that steps in spacing could be discerned reliably from discontinuities in sampling of a smooth topography.

In the first reports of grid cells (Hafting et al. 2005; Fyhn et al. 2007), co-localized cells always had a similar grid orientation (orientation of grid axes), suggesting there was only one shared orientation in the entire circuit. Later work has shown that multiple orientation configurations may be present in the same animal (Krupic et al. 2012; Stensola et al. 2012). The existence of multiple orientation configurations across multiple levels of grid scale highlights a basic question: is the grid map composed of smaller sub-maps or does it act as one coherent representation of space, but with variable geometric features such as spacing and orientation? A grid map with independently functioning sub-maps may produce unique population-pattern combinations for every environment, resulting in unique input patterns to place cells and, in turn, unique hippocampal output (Fyhn et al. 2007). A major objective, based on this possibility, has therefore been to determine if grid cells within the same grid circuit perform separate operations on the same inputs. The next section will address the possibility of a modular functional organization of the grid-cell circuit.

Discretization of the Entorhinal Grid Map

Locally, grid cells behave as a coherent ensemble (Fyhn et al. 2007), but it was unknown from the first reports if the entire grid map functioned as a coordinated whole or if it was fractioned into sub-units that displayed a capacity for independent function. By combining novel and established experimental approaches, we were able to record an unprecedented number of grid cells—up to 186 cells from the same animal—which finally allowed us to determine that the grid map is a conglomerate of sub-maps or modules (Stensola et al. 2012).

The new recordings showed, within animals, that the gradient in grid scale (grid spacing) along the dorsoventral axis of MEC progressed in clear steps rather than as

a continuum. All cells within a module shared the same grid spacing, and modules of increasing scale became more abundant as the tetrodes were turned to more ventral MEC locations. Cells that shared the same grid spacing within animals also had a common grid orientation, defined as the orientation of the grid axes relative to the local boundaries of the environment. Most grid cells also demonstrated small but consistent deviations from perfect hexagonal symmetry, expressed by the fact that the inner ring of fields in the grid pattern formed an ellipse rather than a circle. These deformations were consistent across cells in the same grid module (Stensola et al. 2012). No modular organization was apparent within the population of head direction cells in the MEC (Giocomo et al. 2014).

Modular organization was also expressed in the temporal modulation of spike activity. Grid cells are tuned to the ongoing population activity, manifested as oscillations in the local field potential (Hafting et al. 2008; Jeewajee et al. 2008). Several models implicate theta rhythms in the generation of the grid pattern (Burgess et al. 2007; for review, see Moser et al. 2014). Previous work had shown that cells at ventral locations of the dorsoventral MEC axis oscillated with a slower beat frequency than dorsal cells, and it was suggested that this gradient arose from gradients in the expression of specific ion channels (Giocomo et al. 2007; Giocomo and Hasselmo 2008; Garden et al. 2008; Jeewajee et al. 2008). We found that grid cells in geometrically defined modules were modulated by the same theta frequency. On average, modules with greater grid spacing had lower theta frequencies, but within animals, modules were not strictly confined to this trend.

The consistency of geometric features within but not across modules made it possible to define module membership for all cells with an automated multidimensional clustering approach (K-means clustering). After defining the modules, we could turn to the question of how modules were distributed in the MEC tissue. Several signs of anatomical clustering existed within the entorhinal system (Ikeda et al. 1989; Solodkin and Van Hoesen 1996; Burgalossi et al. 2011), pointing to possible anatomical substrates for the functional clustering. Individual modules occupied extensive portions of MEC. We found that, on average, a module spanned >1 mm of the dorsoventral MEC axis. There was extensive module overlap in the intermediate-to-ventral parts of MEC such that, at any MEC location, cells from several modules could be present. Grid modules were found to cut across cell layers; cells that were part of one module were found in several layers. In contrast to the organization along the dorsoventral axis, there was no discernable topography along the mediolateral axis. Instead, modules extended across large mediolateral distances (~1 mm, which was the limit of our recording arrays), suggesting modules distributed as mediolateral bands along the dorsoventral axis. Based on this knowledge, combined with the distribution of modules along the dorsoventral axis, we could estimate the number of distinct modules within animals to be in the upper single-digit range. This anatomical distribution of modules does not match any known anatomical clustering in the entorhinal cytoarchitecture.

With previous reports having suggested a set relationship between scale steps (Barry et al. 2007), we next quantified the relationship between module scales

within and across animals. Within animals, there was considerable variation in the relationship between one module scale and the next, suggesting that scale is set independently for each module and animal. However, when we pooled the scale progression across animals, a pattern was revealed. On average, modules increased by a fixed scale ratio, as a geometric progression. The mean ratio was 1.42, very close to $\sqrt{2}$. This relationship pointed to genetic circuit-mechanisms as contributors to grid scale, yet the geometric individuality of the modules suggested that modules exhibited a substantial level of autonomy.

Finally, in a separate set of experiments, we tested if grid modules were also functionally independent. Grid cells are known to rescale along with environmental compression (Barry et al. 2007; Solstad et al. 2008). We found that, when animals were exposed to a relocation of one of the walls in the environment, modules rescaled along the compression, but to varying degrees (Stensola et al. 2012). Cells within a module behaved coherently, whereas individual modules could rescale to completely different extents within animals. This finding provided the first proof-of-principle for independent function within sub-populations in the grid map.

Combinatorics in Grid Cells and Remapping in Place Cells

In a landmark study of place cells, Muller and Kubie (1987) described a phenomenon that had great implications for our understanding of the relationship between the spatial map in hippocampus and its role in memory formation. For one, they demonstrated, in agreement with earlier work (O'Keefe and Conway 1978), that place cells were under the control of sensory cues in the environment, as rotation of a cue resulted in consistent rotation of the place fields. More importantly, they showed that, if two recording environments differed beyond a certain magnitude, the activity of the recorded cells changed drastically between the environments. Among the cells that were active in the first environment and remained active in the second, the firing locations were completely reorganized in space. Further, a large portion of cells that were active in one environment became silent in the next. Other cells were active only in the second environment. This functional reorganization was termed 'remapping' and represented an orthogonalization in the population encoding between the distinct environments.

Grid modularity appears to offer very favorable conditions for hippocampal remapping (Fig. 3). Maps from different grid modules could reorganize to yield completely novel downstream population inputs and, therefore, new hippocampal place maps. Early work showed that grid cells realigned with the environment when remapping took place in simultaneously recorded hippocampal place cells (Fyhn et al. 2007). The realignment involved a shift in grid phase and a reorientation of the grid pattern relative to the geometry of the environment. The realignment was coherent for all grid cells recorded, so that spatial relationships between the grid cells remained. This observation does not preclude independent realignment of distinct modules, however, because all of the grid cells in the early work were

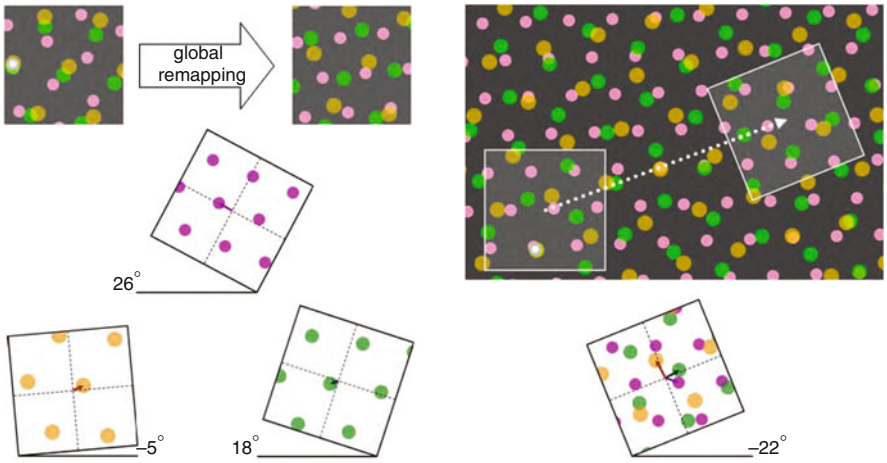

Fig. 3 Two proposed mechanisms that may underlie hippocampal remapping based on grid inputs. *Left*: several independent grid maps, each with a different *color*, realign independently (*bottom*) and cause unique combinatorial population patterns in the hippocampus (*top*). *Right*: the grid map is coherent across scales, and remapping occurs from a shift in spatial phase space. Reproduced with permission from Fyhn et al. (2007)

recorded at the dorsal end of the MEC and all had a relatively similar grid scale, i.e., most of the cells may have belonged to the same module.

If grid modules are the main source of hippocampal remapping, the level of independence between grid modules will affect remapping-based mnemonic capacity. But how independent are the grid modules? Grid modules have several geometric traits that suggest autonomy (Stensola et al. 2012). Grid spacing relationships varied across animals, and grid orientation could be completely offset between modules. Grid modules also differed in the amount and directionality of pattern deformation, and deformation, scale and orientation changed independently across modules when the animal was exposed to a novel room (Fig. 4). These observations are entirely consistent with an attractor mechanism for grid formation. In attractor models of grid cells, a grid network can only support a circuit in which all cells share the same geometry (McNaughton et al. 2006; Burak and Fiete 2009; Moser et al. 2014).

A surprising observation, however, was that modules typically assumed one of only four distinct orientation configurations relative to the environment (Stensola et al. 2015). This constraint on orientation may seem highly disadvantageous for generating maximally distinct hippocampal inputs. However, it has been shown theoretically that remapping based on grid modules is much more sensitive to the spatial phase offset between the modules than the relative orientation and spacing (Monaco and Abbott 2011; Fig. 5). Varying grid orientation caused less reorganization in hippocampus compared to varying phase.

The differences in rescaling across grid modules may shed light on the mechanisms underlying rescaling of hippocampal place fields after changes in the

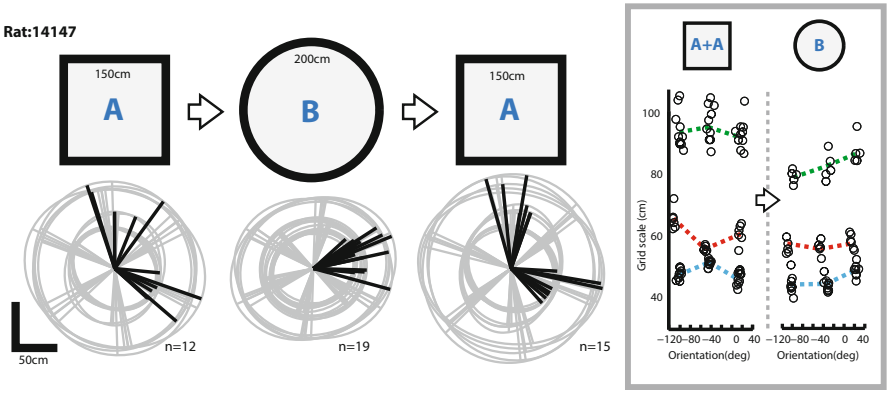

Fig. 4 Modules realigned when animals were tested in a novel box in a novel room. Grid scale, orientation and ellipse directions all changed independently between modules, strongly suggesting independent operations. The *left panel* shows grid axes and ellipse (*gray lines*) and ellipse tilt (*black line*) from all cells in one animal in square and circular environments. Note the independent changes in ellipse tilt. The *figure* on the *right* shows data from all three grid axes in the *square* and the *circle*. Reproduced, with permission, from Stensola et al. (2012)

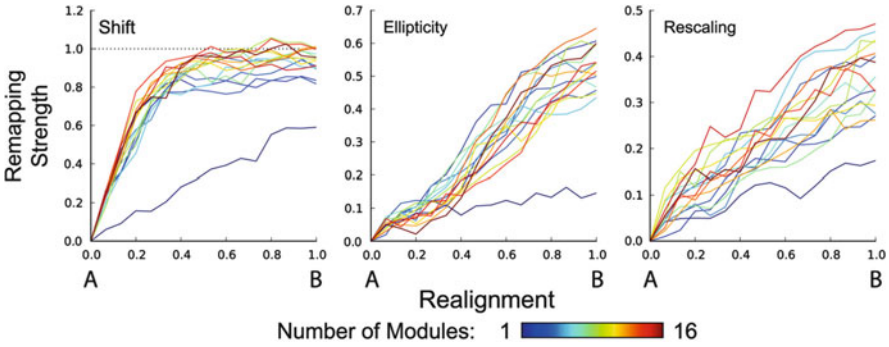

Fig. 5 Efficacy of reorganizing different parameters of grid geometry between modules. The strongest remapping occurred from phase shifts, while other features (changes in elliptic deformation or scale) were less effective. A and B denote the two distinct environments. Reproduced, with permission, from Monaco and Abbott (2011)

geometry of the environment (O'Keefe and Burgess 1996). O'Keefe and Burgess recorded place cells in a rectangular environment that could be extended or compressed in any of the four cardinal directions. When the recording box was extended or compressed, place fields followed the change in environmental geometry. Some cells were anchored to one wall or a set of walls so that their firing fields moved along with the extension. Other cells were anchored to the external room instead of the box, and yet others distended the place field along the box or even split the field in two parts. This behavior suggested an underlying input pattern with a distinct geometric relationship to the walls of the recording box or the room.

Based on their observations, the authors proposed a model in which spatial modulation arose from the sum of multiple Gaussian activity bands offset from the environmental boundaries at different distances (O'Keefe and Burgess 1996). This idea was later developed into the boundary-vector model of place cells (Hartley et al. 2000; Barry et al. 2006). Although boundary-selective cells exist in MEC and do project to hippocampal place cells (Zhang et al. 2013), this study is also intuitively in line with expectations from the observations of grid rescaling. Because of rescaling, place fields can receive input that is topologically identical to the original map, only distended or compressed, likely resulting in distended or compressed place fields. If a place cell receives input from two modules, and these modules differ greatly in rescaling, it seems reasonable to assume that their contribution is split into two fields under some circumstances.

Topography in Parahippocampal Systems

In sensory and motor cortices, there is often a neat correspondence between relationships in the external world and their internal representations in the brain, that is to say, continuous or discrete variables in the external world are mapped topographically into the cortical sheet (Rasmussen and Penfield 1947). Topography often represents a 'where' component onto which information about stimulus quality can be superimposed (Tolman 1948; Montagnini and Treves 2003; Kaas 2012). Similar correspondences are not present in the entorhinal-hippocampal system. Neither place cells nor grid cells display topographic representation of spatial location, at least not at the macroscopic level (O'Keefe 1976; Redish et al. 2001; Hafting et al. 2005). In the hippocampus, with two-photon imaging, the activity of an entire ensemble of hippocampal place cells could be imaged simultaneously while a mouse navigated within a virtual environment (Dombeck et al. 2010; Harvey et al. 2009). The place cells developed clear place fields, suggesting the task was not too alienating for the spatial representation system. Further, there was no statistical relationship between the location of place cells in the hippocampal cellular sheet (>35 μm apart), and the locations of their place fields in virtual space. Cell pairs <35 μm apart, displayed a significant correlation but not separable from correlations from common neuropil or activity bleed-over in the imaging technique (Dombeck et al. 2010). Imaging of grid cells using similar methods has recently confirmed that grid phase is organized non-topographically at the macroscopic level, but larger-than-expected correlations were reported for cells that were nearest neighbors (Heys et al. 2014).

The low level of topography in the adult spatial representation system does not exclude the existence of topography at earlier developmental stages. Mechanisms by which topography is present during development as a teaching signal to set up appropriate circuitry for grid function, only to disappear in the adult brain, have been proposed for place cells (Samsonovich and McNaughton 1997) as well as grid cells (McNaughton et al. 2006). It is worth noting that both hippocampus and

entorhinal cortex are evolutionarily 'old,' such that the orderly topography seen in typical low level cortex only likely arose after these structures were past their phylogenetic window of opportunity (Kaas 2012). The olfactory piriform cortex is another ancient cortical structure that does not show topographical organization, even though continuity in stimulus dimensions exists and similar teaching inputs may have been present.

The apparent lack of topographical mapping of firing locations contrasts with the progressive increase in average scale of place cells (Jung et al. 1994; Kjelstrup et al. 2008) and grid cells (Fyhn et al. 2004; Hafting et al. 2005; Brun et al. 2008) along the dorsoventral axis of the hippocampus and the MEC, respectively. What are the functional consequences of this scale expansion? There is an extensive literature on the distinct features of dorsal and ventral portions of the hippocampus. Lesions at different dorsoventral portions produce markedly different behavioral deficits (Nadel 1968; Moser et al. 1993). Lesions of a small portion of the dorsal pole impair spatial memory efficiently, whereas similar portions of the ventral pole do not (Moser et al. 1993, 1995). Stress responses and emotional behavior are affected by lesions to ventral but not dorsal portions of hippocampus (Henke 1990; Kjelstrup et al. 2002). Connectivity to and from these portions of hippocampus is distinct (Witter et al. 1989; Dolorfo and Amaral 1998). There is also a growing body of literature in spatial cognition in humans suggesting functional polarization along the human equivalent of the dorsoventral axis (Fanselow and Dong 2010; Poppenk et al. 2013). In particular, activity in the human equivalent of the ventral hippocampus is associated with coarse global spatial representations and route planning and execution, whereas the dorsal equivalent is associated with fine-grained local representations and navigation strategies, such as number of turns on a route (Evensmoen et al. 2013).

The neural codes along the dorsoventral axis of the parahippocampal spatial system may very well reflect an axis of generalization. With increased scale of spatial fields in the hippocampus and the MEC, the larger fields do not denote spatial location with equal demarcation, so spatial resolution is diminished. Another consequence is that for these ventral codes, at any particular point in space, a greater portion of cells will be active. This increase in representational density may confer better robustness to noise: the more cells that can take part in a 'majority' vote, the better the vote will be statistically, despite poorer spatial resolution. Exactly the same argument can be made for the representation of head direction, whose resolution also decreases from dorsal to ventral MEC (Giocomo et al. 2014; Fig. 6). Alternatively, ventral cells (both grid, place and head direction cells) code a larger portion of the environment at any moment, so that the population code at any location is more generalized. This may be beneficial for associating content into current spatial contexts. The ventral hippocampus is more associated with stress and fear responses and has stronger connections with the amygdala (Moser and Moser 1998). For embedding fear memories into spatial context, it may be advantageous to impose a higher level of generalization.

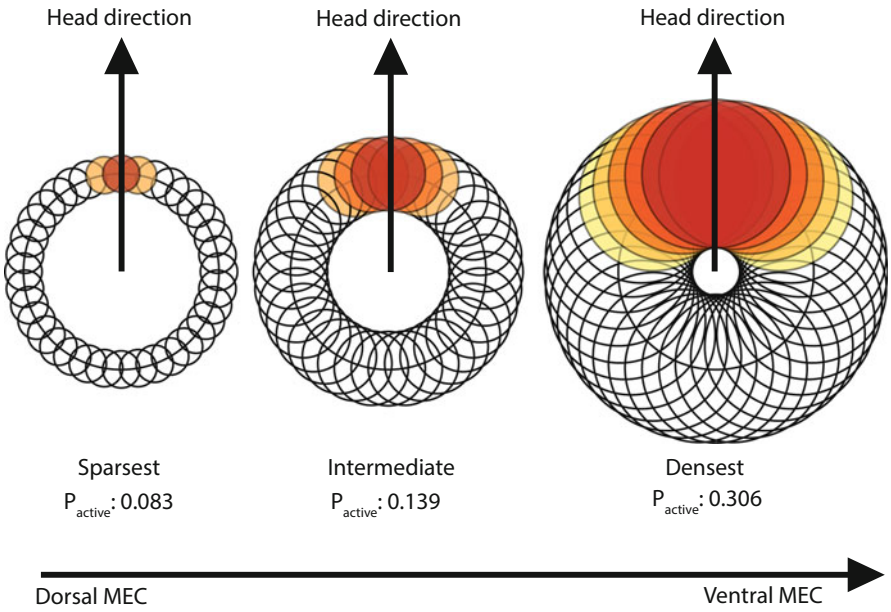

Fig. 6 Head direction representational density increases along the dorsoventral axis in MEC layer 3. Each doughnut represents a head direction cell population, and each cell is represented as a *circle* on the doughnut. The location and size of the *circle* represent preferred head direction and tuning specificity, respectively. Given populations of equal size (same number of rings; dorsal to ventral as *left* to *right*), and the same directional input, ventral populations will have a larger proportion (P) of its cell population be active to any input compared to more dorsal populations due to broader tuning (*color* gradient shows each cell's activity level; *red* is maximum)

Mechanisms of Grid Spacing

Our studies have shown that grid spacing increases in steps along the dorsoventral axis of MEC. The factors that determine topographical grid spacing are currently unknown. When all module pair ratios were pooled across animals, a consistent average scale ratio was revealed. This consistency across animals implies a genetic component in determining grid spacing. Gradients of specific ion channels, such as the hyperpolarization-activated cyclic nucleotide-gated (HCN) channels, exist in entorhinal cortex and have been suggested to account for the topography of grid scale (Giocomo et al. 2007, Giocomo and Hasselmo 2009; Garden et al. 2008). However, such channels, when genetically knocked out, did not remove grid scaling along the dorsoventral axis but instead changed the baseline spacing (Giocomo et al. 2011). Other channel gradients may contribute to scaling, such as potassium channels (Garden et al. 2008). If scale is determined in part from channel gradients, or indeed any genetic expression pattern, it seems likely the gradient will provide a smooth topography of any conferred scale parameter, instead of a

modular organization. How then could modular grid scale result from a smooth underlying gradient?

One possible scenario is that module grid scale is determined by network dynamics acting on a graded underlying scale parameter. Attractor models of grid cells predict that all cells in a circuit must have the same grid spacing (as well as orientation and pattern deformation) to generate a stable grid pattern (Welinder et al. 2008). Within a grid network determined by attractor dynamics, there will likely be some tolerance to small variations in the scale-parameter distribution across cells, so that when the network is initiated, the effects of population dynamics dominate individual cells enough to coordinate all cells into a common pattern, cancelling out individual variation. In a sense, this 'spatial synchronization' acts similarly to synchronization in the temporal domain; originally observed by Huygens in 1665, coupled oscillators settle on a mean frequency that entrains all the individual oscillators, even in the presence of relatively large variations in individual frequencies. But what would happen if the scale parameter distribution exhibits too large spread? The variation may become too large to entrain all units into one coherent pattern, and the pattern may fraction into sub-ensembles that each center on a mean frequency that the ensemble can sustain. This way, by having a network self-organize from a very wide, continuous scale parameter distribution, such as channel expressions along an axis in MEC, several local modules of internal spatial consistency could arise from the unstable global pattern.

We observed convincing signs of independence between modules within animals, in terms of pattern geometry and rescaling responses. To incorporate this finding into the suggested mechanism above, one can suppose that, during development, learning strengthens connections within spatially synchronized ensembles but weakens connections between spatially desynchronized cells. In agreement with this possibility, grid cell pairs with similar spatial phase show stronger functional connectivity than pairs with dissimilar phase (Dunn et al. 2015). If two cells have a similar spatial phase, their coordinated firing in space will cause coordinated firing in time, a prerequisite for many forms of long-term potentiation (LTP; Bi and Poo 1998). Enhancement of connections between grid cells with a similar phase would lead to the development of functional ensembles intermingled in the same tissue, with strong inter-ensemble connectivity and weak cross-ensemble connectivity, in effect decoupling the ensembles functionally. A testable prediction from this idea is that very young animals, which have yet to achieve complete module decoupling, will display grid cells with poor spatial regularity because the network cannot sustain a coherent grid pattern based on cross-ensemble interactions. As the animal explores more space, decoupling will at some point become complete enough for cells to self-organize into modules with coherent and regular grid patterns. Such a transition may be rapid, as it may involve a 'tipping point' after which network dynamics kick in to entrain the ensemble. In two studies that characterized grid cells in early development in rats, grid patterns were indeed not very regular initially (Langston et al. 2010; Wills et al. 2010). Only at the age of about 4 weeks, 1–2 weeks after the beginning of outbound exploration, did regular

grid firing occur. The transition to this state had a rapid onset, in line with the above proposal.

Conversely, if the scale parameter is associated with temporal characteristics such as intrinsic resonance frequency, as suggested in several models (Burgess et al. 2007) and by experimental findings (Giocomo et al. 2007, 2011; Jeewajee et al. 2008), synchronization in the temporal domain during development could result in similar module fractionation and synaptic modification to cause *temporally* consistent ensembles. If the scale parameter is associated with temporal frequency, these temporally synchronized ensembles would also become spatially synchronized. By this mechanism, grid modules could develop to mature, functionally decoupled modules at least in part before the animal ever explores space. In line with this is our finding that modules are temporally consistent.

Shearing-Induced Asymmetries in Grid Cells

There are no hexagonal features in the environment that correspond to the grid pattern. Grid patterns are instead believed to arise from local network dynamics, with self-motion input as a major update mechanism (Fuhs and Touretzky 2006; McNaughton et al. 2006; Welinder et al. 2008; Couey et al. 2013). However, for the grid pattern to be useful in allocentric representations, it must anchor to the external environment. Several features of the pattern could be involved in this anchoring process, including spatial phase (offset in the x, y-plane), grid spacing and grid orientation (alignment between grid axes and axes of the environment). We demonstrated earlier that grid orientation can assume distinct orientations across and within animals (Stensola et al. 2012), but it was unknown whether there was any orderly relationship between grid alignment and specific features of the environment.

In a recent study (Stensola et al. 2015), we compared grid orientation from large data sets recorded in two distinct square environments, enabling rigorous analyses of grid alignment. Grid orientation did not distribute randomly across animals. Instead, there was a strong tendency for grid axes to align to the cardinal axes of the environment, defined by the walls of the recording enclosure. In one environment, we observed clustering around one wall axis only, whereas in the other environment grid orientation distributed around both cardinal axes. The strong bias towards the box axes suggested the box geometry itself acted as the grid anchor, and not salient extra-environmental visual cues, which were deliberately abundant.

Rather than aligning parallel to the box axes, cells were consistently offset from these axes by a small amount in all environments. In one environment, this offset was to either side of one cardinal axis. In the second environment, cells were also offset from parallel, but with reference to both cardinal axes. The rotation was identical across the two environments; cells were systematically offset from parallel by 7.5°, with a standard deviation of 2–3°, yielding four general alignment configurations for square environments. The observed distributions were not a result of

pooling across cells from different modules, as individual grid modules expressed the same absolute offset configurations, i.e., 7.5°.

What could be the function of the consistent offset of the grid axes? We noted that a triangular pattern within a square is maximally asymmetric at 7.5° rotation in relation to the axes of symmetry in the square, the same as the offset observed in the data. The environmental axes are primarily available to the animal in the form of borders imposed by the walls of the environment. Because border segments have been implicated in spatial coding (O'Keefe and Burgess 1996; Hartley et al. 2000; Barry et al. 2006) and because MEC contains cells that encode these specifically (Solstad et al. 2008; Savelli et al. 2008), we hypothesized that one function performed by grid alignment is to create maximally distinct population codes along border segments of the environment. This may be critical for encoding environments in which sensory input is ambiguous. Grid cells are thought to perform path integration (dead-reckoning from integration of distance and angle over time) based on self-motion cues. Without occasional sensory input, however, errors will accumulate until the representation becomes entirely unreliable. Sensory cues affect grid cells (Hafting et al. 2005; Savelli et al. 2008) and are thought to provide update signals that recalibrate path integration and reset accumulated errors. The symmetry and geometric ambiguity of the square recording environment may render such sensory cues less useful because multiple locations in the environment may produce similar update signals at different absolute locations. Therefore, error may be minimized by orientation solutions that maximize the distinctness of population representations at ambiguous locations.

Closer inspection showed that the angular offset of the grid axes differed between grid axes and depended on the angular distance from any of the walls of the square environment (Stensola et al. 2015). The further away a grid axis was from any of the walls, the smaller was the angular offset. The differential offset gave rise to an elliptic deformation of the circle described by the inner six fields of the grid pattern. The size and orientation of this elliptic deformation was not randomly distributed. In particular, the angular difference between the ellipse orientation of modules was clustered around 90 or 0° (Stensola et al. 2012). Because of this apparent link to the square geometry of the box geometry, we were inclined to investigate any possible links between elliptification of the grid and its offset. Ellipse orientation correlated strongly with angular offset, leading us to hypothesize that grid deformation and offset were the result of a common underlying process.

In continuum mechanics, simple shearing is a geometric transform that displaces points on a plane along a shear axis. Any point is displaced by an amount directly proportional to its Euclidian distance to that shear axis. The effect of this transformation on points that lie on a circle is that the circle becomes elliptic. Further, any axis on this circle will display non-coaxial rotation, the magnitude of which is directly proportional to the angular distance from the shear axis. To determine whether shearing could account jointly for the elliptic deformation and the angular offset of the grid, we applied shearing transformations to all grid patterns, with either of the cardinal box-wall axes as the shear axis (Stensola et al. 2015). Each

grid was sheared along each wall axis until it was minimally deformed, that is, least elliptical. We then determined how much the transform managed to reduce deformation, and how much the rotational offset was changed. We performed separate analyses for differently sized recording environments.

In the 1.5-m box, simple shearing removed most of the deformation (ellipticity was reduced from 1.17 to 1.06). It further completely removed the bimodal 7.5° offset peaks. The offset distribution became unimodal, with a peak centered close to 0° (parallel to one of the wall axes). This robust explanatory power of *simple* shearing implies that the grid pattern is globally anchored to one set of features such as a wall or a corner. We hypothesized that shearing develops with experience. In a smaller data set taken from a previous study (Fyhn et al. 2007), offset was indeed significantly closer to parallel in novel environment exposures than in familiar ones.

The 2.2-m box had more than twice the area of the 1.5-m box. Maintaining a coherent grid pattern may be sensitive to excessive distances between environmental features. If grid anchoring is globally set by a single feature (e.g., a border or wall), as suggested above, the integrity of the grid pattern may suffer at distances far from such anchoring points. We have shown previously that grid patterns fragment into local patterns in complex environments (Derdikman et al. 2009). We reasoned that, as the environment becomes larger, the grid pattern will benefit from stabilization by multiple anchoring points. In sufficiently large environments, spatial representation might break into locally anchored patterns that merge in the interior of the environment.

We applied simple shearing transforms to all grids from the 2.2-m box, exactly as with the smaller box. Minimizing deformation reduced ellipticity to the same extent, but the rotational offset was only partially removed. To test whether shearing occurred simultaneously from both wall axes, we determined for each cell the minimal deformation possible with a two-axis shearing transform. We could detect exactly one such minimum for every cell, suggesting it was one-to-one in the domain we were exploring. We then, as above, analyzed the impact on rotational offsets. The two-axis transform completely removed the offset peaks in the 2.2-m box, suggesting that the grid pattern had been sheared from two distinct anchoring sites.

A few modules did not display the common 7.5° offset and were not amenable to offset reduction through shearing. These modules nonetheless had 7.5° offsets locally in particular areas of the box. Such local offsets might not be detectable in a spatial autocorrelogram as the latter captures global pattern regularities. The distinct local grid patterns merged either abruptly or smoothly in the box interior. To quantify the amount of local pattern variation, we compared cross-correlations between quadrants in the 2.2-m box and the 1.5-m box. We could successfully capture the grid geometry in these smaller segments because we generated average quadrant autocorrelograms (from splitting each rate map into equal 2×2 sections) for each module. Cross-correlations were much higher in the 1.5-m box compared to the 2.2-m box, supporting the notion that the larger box induced local and more complex anchoring.

Finally, we performed the same analyses on the 2.2-m box data but with rate maps divided into 3×3 segments. There were clear differences in deformation patterns across these segments. Grid scores (rotational symmetry) were significantly higher in the central bin compared to the peripheral bins. Corner segments showed a particularly high degree of deformation, and in one corner—the corner where all animals were released into the box—ellipse direction showed a remarkably low degree of variation.

The need to anchor internal representations of space to external frames is paramount for allocentric function. We have demonstrated that grids align to the environment in a systematic manner. We have also suggested that the alignment of the grid pattern can be used to counteract mislocation within geometrically ambiguous environments. Rats tested in spatial working memory tasks in rectangular environments make systematic errors in segments of the box that have rotationally equivalent geometry, even in the presence of polarizing cues (Cheng 1986), which suggests geometric confusion is a common issue in spatial representation, as is supported by similar effects found in several other species (Cheng 2008).

We hypothesize that border cells provide mechanistic links between the grid map and the external environment. Despite abundant visual landmarks in the recording rooms, modules, with few exceptions, aligned according to the geometry of the environment. There may be a special salience given to environment borders, as opposed to more point-like visual cues, because environmental borders are generally more dependable and have an orientation. Biegler and Morris (1993) found that rats only used landmarks within an environment to gauge distances if the landmarks were stable within that environment. Several studies have shown similar connections to environmental geometry in other cell types (Save et al. 2000; Knierim et al. 1995, 1998; Sharp et al. 1995; Etienne et al. 2004) but have also highlighted the fact that the system's use of landmarks for spatial representation can be changed experimentally through learning (Jeffery et al. 1997). The close match between observed alignment and the alignment that would maximally decorrelate population codes across segments of the environment suggests that there could be a competitive interaction between path integration signals and sensory resets, as observed previously for place cells in the hippocampus (Gothard et al. 1996; Redish et al. 2000).

Oblique Effect in Grids?

Discrimination and detection of visual stimuli are dependent on the relationship of the stimulus to the axes of the environment, a well-known effect known as the 'oblique effect' (Mach 1860). Stimuli oriented along the cardinal axes yield better psychophysical performance compared to obliquely oriented stimuli. In the visual cortices, both single-neuron responses and population responses reflect this psychophysical anisotropy by increased representational density along the cardinal axes (Furmanski and Engel 2000; Wang et al. 2003; Xu et al. 2006). Several studies

suggest that the oblique effect originates in higher order cortices (Nasr and Tootell 2012; Liang et al. 2007; Shen et al. 2008), as the effect is stronger here compared to early sensory cortex (Shen et al. 2008; Müller et al. 2000), and the effect in early cortex is selectively abolished by temporal inactivation of higher order cortex (Shen et al. 2008). Grid cells are typically aligned close to parallel to the cardinal axes of the environment. Recently, it was shown that grid representations are not limited to navigational space in that a grid map of visual space was demonstrated in the entorhinal cortex of monkeys (Killian et al. 2012). Although highly speculative, it is interesting to ponder the possibilities for similar mechanisms at play in embedding internal representations into external reference frames in the visual domain as in the spatial domain. Although not very many examples were given by Killian et al. (2012), there seems to also be a trend for grids to align with a slight offset to cardinal axes (see their Fig. 1). Further, using optical imaging in area MT (which shows movement and orientation selectivity for stimuli) in the visual system, Xu et al. (2006) showed frequency plots of activation over the range of possible stimulus orientations. In these plots, there are quite distinct peaks with bimodal offsets from the cardinal axes (Fig. 7). Upon further inspection, these offsets are very close to 7.5°, which is the exact peak we observed in the alignment offset in grid cells. This finding points to a possible, albeit suppositional, link between visual

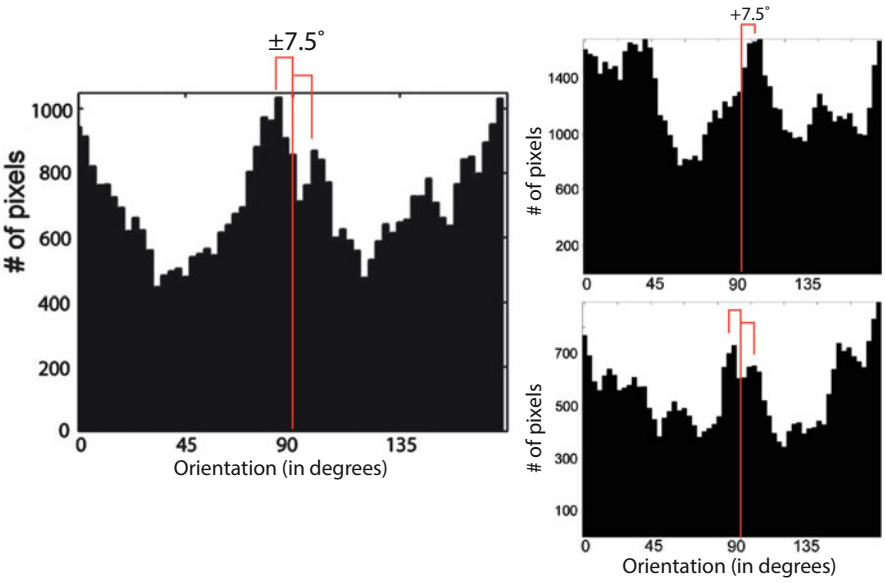

Fig. 7 The oblique effect in visual area MT in the owl monkey. Histograms show local activity measured by intrinsic optical imaging. Increased pixel count (y-axis) corresponds to higher activation. The different panels are from distinct subareas within MT. The *red lines* show 7.5° offsets calculated from the x-axis of the plots. Note the correspondence between peak offset and *red lines*. Reproduced with permission from Xu et al. (2006) (their Fig. 3 and Supplementary Fig. 6)

and spatial encoding in relation to real world axes, a link to be explored through future studies.

Conclusions

The entorhinal-hippocampal circuit offers a good model system for investigating basic functions carried out by neural networks within a behavioral context. Our understanding of grid cells has developed substantially at the single cell level but has for a while lagged behind the population insights gained from the hippocampus. By overcoming technical and analytic hurdles, we have now defined the first large-scale population characteristics of two central space-encoding cell populations. The grid map was shown to be modular, with considerable independence in the response of modules to geometrical features of the environment. Grid modules were found to use a general strategy to anchor grid orientation to the environment, pointing to this strategy as an optimal mechanism for population encoding of ambiguous segments of the external environment.

References

Barry C, Lever C, Hayman R, Hartley T, Burton S, O'Keefe J, Jeffery K, Burgess N (2006) The boundary vector cell model of place cell firing and spatial memory. Rev Neurosci 17:71–97

Barry C, Hayman R, Burgess N, Jeffery KJ (2007) Experience-dependent rescaling of entorhinal grids. Nat Neurosci 10:682–684

Bi GQ, Poo MM (1998) Synaptic modifications in cultured hippocampal neurons: dependence on spike timing, synaptic strength, and postsynaptic cell type. J Neurosci 18:10464–10472

Biegler R, Morris RG (1993) Landmark stability is a prerequisite for spatial but not discrimination learning. Nature 361:631–633

Brun VH, Otnass MK, Molden S, Steffenach HA, Witter MP, Moser MB, Moser EI (2002) Place cells and place recognition maintained by direct entorhinal-hippocampal circuitry. Science 296:2243–2246

Brun VH, Solstad T, Kjelstrup KB, Fyhn M, Witter MP, Moser EI, Moser MB (2008) Progressive increase in grid scale from dorsal to ventral medial entorhinal cortex. Hippocampus 18:1200–1212

Burak Y, Fiete IR (2009) Accurate path integration in continuous attractor network models of grid cells. PLoS Comput Biol 5:e1000291

Burgalossi A, Herfst L, von Heimendahl M, Forste H, Haskic K, Schmidt M, Brecht M (2011) Microcircuits of functionally identified neurons in the rat medial entorhinal cortex. Neuron 70:773–786

Burgess N, Barry C, O'Keefe J (2007) An oscillatory interference model of grid cell firing. Hippocampus 17:801–812

Cheng K (1986) A purely geometric module in the rat's spatial representation. Cognition 23:149–178

Cheng K (2008) Whither geometry? Troubles of the geometric module. Trends Cogn Sci 12:355–361

Couey JJ, Witoelar A, Zhang SJ, Zheng K, Ye J, Dunn B, Czajkowski R, Moser MB, Moser EI, Roudi Y, Witter MP (2013) Recurrent inhibitory circuitry as a mechanism for grid formation. Nat Neurosci 16:318–324

Derdikman D, Whitlock JR, Tsao A, Fyhn M, Hafting T, Moser MB, Moser EI (2009) Fragmentation of grid cell maps in a multicompartment environment. Nat Neurosci 12:1325–1332

Dolorfo CL, Amaral DG (1998) Entorhinal cortex of the rat: topographic organization of the cells of origin of the perforant path projection to the dentate gyrus. J Comp Neurol 398:25–48

Dombeck DA, Harvey CD, Tian L, Looger LL, Tank DW (2010) Functional imaging of hippocampal place cells at cellular resolution during virtual navigation. Nat Neurosci 13:1433–1440

Dunn B, Mørreaunet M, Roudi Y (2015) Correlations and functional connections in a population of grid cells. PLoS Comput Biol 11:e1004052

Etienne AS, Maurer R, Boulens V, Levy A, Rowe T (2004) Resetting the path integrator: a basic condition for route-based navigation. J Exp Biol 207:1491–1508

Evensmoen HR, Lehn H, Xu J, Witter MP, Nadel L, Håberg AK (2013) The anterior hippocampus supports a coarse, global environmental representation and the posterior hippocampus supports fine-grained, local environmental representations. J Cogn Neurosci 25:1908–1925

Fanselow MS, Dong H-W (2010) Are the dorsal and ventral hippocampus functionally distinct structures? Neuron 65:7–19

Fuhs MC, Touretzky DS (2006) A spin glass model of path integration in rat medial entorhinal cortex. J Neurosci 26:4266–4276

Furmanski CS, Engel SA (2000) An oblique effect in human primary visual cortex. Nat Neurosci 3:535–536

Fyhn M, Molden S, Witter MP, Moser EI, Moser M-B (2004) Spatial representation in the entorhinal cortex. Science 305:1258–1264

Fyhn M, Hafting T, Treves A, Moser M-B, Moser EI (2007) Hippocampal remapping and grid realignment in entorhinal cortex. Nature 446:190–194

Garden DL, Dodson PD, O'Donnell C, White MD, Nolan MF (2008) Tuning of synaptic integration in the medial entorhinal cortex to the organization of grid cell firing fields. Neuron 60:875–889

Giocomo LM, Hasselmo ME (2008) Time constants of h current in layer ii stellate cells differ along the dorsal to ventral axis of medial entorhinal cortex. J Neurosci 28:9414–9425

Giocomo LM, Hasselmo ME (2009) Knock-out of HCN1 subunit flattens dorsal-ventral frequency gradient of medial entorhinal neurons in adult mice. J Neurosci 29:7625–7630

Giocomo LM, Zilli EA, Fransén E, Hasselmo ME (2007) Temporal frequency of subthreshold oscillations scales with entorhinal grid cell field spacing. Science 315:1719–1722

Giocomo LM, Hussaini SA, Zheng F, Kandel ER, Moser MB, Moser EI (2011) Grid cells use HCN1 channels for spatial scaling. Cell 147:1159–1170

Giocomo LM, Stensola T, Bonnevie T, Van Cauter T, Moser M-B, Moser EI (2014) Topography of head direction cells in medial entorhinal cortex. Curr Biol 24:252–262

Gothard KM, Skaggs WE, McNaughton BL (1996) Dynamics of mismatch correction in the hippocampal ensemble code for space: interaction between path integration and environmental cues. J Neurosci 16:8027–8040

Hafting T, Fyhn M, Molden S, Moser M-B, Moser EI (2005) Microstructure of a spatial map in the entorhinal cortex. Nature 436:801–806

Hafting T, Fyhn M, Bonnevie T, Moser M-B, Moser EI (2008) Hippocampus-independent phase precession in entorhinal grid cells. Nature 453:1248–1252
Hargreaves EL, Rao G, Lee I, Knierim JJ (2005) Major dissociation between medial and lateral entorhinal input to dorsal hippocampus. Science 308:1792–1794
Hartley T, Burgess N, Lever C, Cacucci F, O'Keefe J (2000) Modeling place fields in terms of the cortical inputs to the hippocampus. Hippocampus 10:369–379
Harvey CD, Collman F, Dombeck DA, Tank DW (2009) Intracellular dynamics of hippocampal place cells during virtual navigation. Nature 461:941–946
Henke PG (1990) Hippocampal pathway to the amygdala and stress ulcer development. Brain Res Bull 25:691–695
Heys JG, Rangarajan KV, Dombeck DA (2014) The functional micro-organization of grid cells revealed by cellular-resolution imaging. Neuron 84:1079–1090
Ikeda J, Mori K, Oka S, Watanbe Y (1989) A columnar arrangement of dendritic processes of entorhinal cortex neurons revealed by a monoclonal antibody. Brain Res 505:176–179
Jeewajee A, Barry C, O'Keefe J, Burgess N (2008) Grid cells and theta as oscillatory interference: electrophysiological data from freely moving rats. Hippocampus 18:1175–1185
Jeffery KJ, Donnett JG, Burgess N, O'Keefe JM (1997) Directional control of hippocampal place fields. Exp Brain Res 117:131–142
Jung MW, Wiener SI, McNaughton BL (1994) Comparison of spatial firing characteristics of units in dorsal and ventral hippocampus of the rat. J Neurosci 14:7347–7356
Kaas JH (2012) Evolution of columns, modules, and domains in the neocortex of primates. Proc Natl Acad Sci USA 109(Suppl):10655–10660
Killian NJ, Jutras MJ, Buffalo EA (2012) A map of visual space in the primate entorhinal cortex. Nature 491:761–764
Kjelstrup KG, Tuvnes FA, Steffenach HA, Murison R, Moser EI, Moser MB (2002) Reduced fear expression after lesions of the ventral hippocampus. Proc Natl Acad Sci USA 99:10825–10830
Kjelstrup KB, Solstad T, Brun VH, Hafting T, Leutgeb S, Witter MP, Moser EI, Moser MB (2008) Finite scale of spatial representation in the hippocampus. Science 321:140–143
Knierim JJ, Kudrimoti HS, McNaughton BL (1995) Place cells, head direction cells, and the learning of landmark stability. J Neurosci 15:1648–1659
Knierim JJ, Kudrimoti HS, McNaughton BL (1998) Interactions between idiothetic cues and external landmarks in the control of place cells and head direction cells. J Neurophysiol 80:425–446
Krupic J, Burgess N, O'Keefe J (2012) Neural representations of location composed of spatially periodic bands. Science 337:853–857
Langston RF, Ainge JA, Couey JJ, Canto CB, Bjerknes TL, Witter MP, Moser EI, Moser MB (2010) Development of the spatial representation system in the rat. Science 328:1576–1580
Liang Z, Shen W, Shou T (2007) Enhancement of oblique effect in the cat's primary visual cortex via orientation preference shifting induced by excitatory feedback from higher-order cortical area 21a. Neuroscience 145:377–383
Mach E (1860) Ueber das Sehen von Lagen und Winkeln durch die Bewegung des Auges. Sitzungsberichte der Math Cl der Kais Akad der Wissenschaften 42:215–224
McNaughton BL, Battaglia FP, Jensen O, Moser EI, Moser MB (2006) Path integration and the neural basis of the 'cognitive map'. Nat Rev Neurosci 7:663–678
Monaco JD, Abbott LF (2011) Modular realignment of entorhinal grid cell activity as a basis for hippocampal remapping. J Neurosci 31:9414–9425
Montagnini A, Treves A (2003) The evolution of mammalian cortex, from lamination to arealization. Brain Res Bull 60:387–393
Moser MB, Moser EI (1998) Functional differentiation in the hippocampus. Hippocampus 8:608–619
Moser E, Moser M-B, Andersen P (1993) Spatial learning impairment parallels the magnitude of dorsal hippocampal lesions, but is hardly present following ventral lesions. J Neurosci 13:3916–3925

Moser M-B, Moser EI, Forrest E, Andersen P, Morris RG (1995) Spatial learning with a minimslab in the dorsal hippocampus. Proc Natl Acad Sci USA 92:9697–9701
Moser EI, Roudi Y, Witter MP, Kentros C, Bonhoeffer T, Moser MB (2014) Grid cells and cortical representation. Nat Rev Neurosci 15:466–481
Muller RU, Kubie JL (1987) The effects of changes in the environment on the spatial firing of hippocampal complex-spike cells. J Neurosci 7:1951–1968
Müller T, Stetter M, Hübener M, Sengpiel F, Bonhoeffer T, Gödecke I, Chapman B, Löwel S, Obermayer K (2000) An analysis of orientation and ocular dominance patterns in the visual cortex of cats and ferrets. Neural Comput 12:2573–2595
Nadel L (1968) Dorsal and ventral hippocampal lesions and behavior. Physiol Behav 3:891–900
Nasr S, Tootell RB (2012) A cardinal orientation bias in scene-selective visual cortex. J Neurosci 32:14921–14926
O'Keefe J (1976) Place units in the hippocampus of the freely moving rat. Exp Neurol 51:78–109
O'Keefe J, Burgess N (1996) Geometric determinants of the place fields of hippocampal neurons. Nature 381:425–428
O'Keefe J, Burgess N (2005) Dual phase and rate coding in hippocampal place cells: theoretical significance and relationship to entorhinal grid cells. Hippocampus 15:853–866
O'Keefe J, Conway FH (1978) Hippocampal place units in the freely moving rat: why they fire where they fire. Exp Brain Res 31:573–590
O'Keefe J, Dostrovsky J (1971) The hippocampus as a spatial map. Preliminary evidence from unit activity in the freely-moving rat. Brain Res 34:171–175
O'Keefe J, Nadel L (1978) The hippocampus as a cognitive map. Oxford University Press, Oxford
Poppenk J, Evensmoen HR, Moscovitch M, Nadel L (2013) Long-axis specialization of the human hippocampus. Trends Cogn Sci 17:230–240
Rasmussen T, Penfield W (1947) The human sensorimotor cortex as studied by electrical stimulation. Fed Proc 6:184
Redish AD, Rosenzweig ES, Bohanick JD, McNaughton BL, Barnes CA (2000) Dynamics of hippocampal ensemble activity realignment: time versus space. J Neurosci 20:9298–9309
Redish AD, Battaglia FP, Chawla MK, Ekstrom AD, Gerrard JL, Lipa P, Rosenzweig ES, Worley PF, Guzowski JF, McNaughton BL, Barnes CA (2001) Independence of firing correlates of anatomically proximate hippocampal pyramidal cells. J Neurosci 21:RC134
Samsonovich A, McNaughton BL (1997) Path integration and cognitive mapping in a continuous attractor neural network model. J Neurosci 17:5900–5920
Save E, Nerad L, Poucet B (2000) Contribution of multiple sensory information to place field stability in hippocampal place cells. Hippocampus 10:64–76
Savelli F, Yoganarasimha D, Knierim JJ (2008) Influence of boundary removal on the spatial representations of the medial entorhinal cortex. Hippocampus 18:1270–1282
Sharp E, Blair HT, Etkin D, Tzanetos B (1995) Influences of vestibular and visual motion information on the spatial firing patterns of hippocampal place cells. J Neurosci 15:173–189
Shen W, Liang Z, Shou T (2008) Weakened feedback abolishes neural oblique effect evoked by pseudo-natural visual stimuli in area 17 of the cat. Neurosci Lett 437:65–70
Solodkin A, Van Hoesen GW (1996) Entorhinal cortex modules of the human brain. J Comp Neurol 365:610–617
Solstad T, Boccara CN, Kropff E, Moser M-B, Moser EI (2008) Representation of geometric borders in the entorhinal cortex. Science 322:1865–1868
Stensola H, Stensola T, Solstad T, Frøland K, Moser MB, Moser EI (2012) The entorhinal grid map is discretized. Nature 492:72–78
Stensola T, Stensola H, Moser M-B, Moser EI (2015) Shearing-induced asymmetry in entorhinal grid cells. Nature 518:207–212
Tolman EC (1948) Cognitive maps in rats and men. Psychol Rev 55:189–208
Van Cauter T, Poucet B, Save E (2008) Unstable CA1 place cell representation in rats with entorhinal cortex lesions. Eur J Neurosci 27:1933–1946
Wang G, Ding S, Yunokuchi K (2003) Difference in the representation of cardinal and oblique contours in cat visual cortex. Neurosci Lett 338:77–81

Welinder PE, Burak Y, Fiete IR (2008) Grid cells: the position code, neural network models of activity, and the problem of learning. Hippocampus 18:1283–1300

Wills TJ, Cacucci F, Burgess N, O'Keefe J (2010) Development of the hippocampal cognitive map in preweanling rats. Science 328:1573–1576

Wilson MA, McNaughton BL (1993) Dynamics of the hippocampal ensemble code for space. Science 261:1055–1058

Witter MP, Groenewegen HJ, Lopes da Silva FH, Lohman AH (1989) Functional organization of the extrinsic and intrinsic circuitry of the parahippocampal region. Prog Neurobiol 33:161–253

Xu X, Collins CE, Khaytin I, Kaas JH, Casagrande VA (2006) Unequal representation of cardinal vs. oblique orientations in the middle temporal visual area. Proc Natl Acad Sci USA 103:17490–17495

Zhang SJ, Ye J, Miao C, Tsao A, Cerniauskas I, Ledergerber D, Moser MB, Moser EI (2013) Optogenetic dissection of entorhinal-hippocampal functional connectivity. Science 340:1232627